

THE EQUATION OF STATE FOR STELLAR ENVELOPES. II. ALGORITHM AND SELECTED RESULTS

DIMITRI MIHALAS

Department of Astronomy, University of Illinois, and High Altitude Observatory, National Center for Atmospheric Research¹

WERNER DÄPPEN

High Altitude Observatory, National Center for Atmospheric Research

AND

D. G. HUMMER²

Institut für Astronomie und Astrophysik der Universität München

Received 1987 February 2; accepted 1988 February 16

ABSTRACT

We discuss a free-energy-minimization method for computing the dissociation and ionization equilibrium of a multicomponent gas. The adopted free energy includes terms representing the translational free energy of atoms, ions, and molecules; the internal free energy of particles with excited states; the free energy of a partially degenerate electron gas; and the configurational free energy from shielded Coulomb interactions among charged particles.

Internal partition functions are truncated using an occupation probability formalism that accounts for perturbations of bound states by both neutral and charged perturbers. The entire theory is analytical and differentiable to all orders, so it is possible to write explicit analytical formulae for all derivatives required in a Newton-Raphson iteration; these are presented to facilitate future work.

Some representative results for both Saha and free-energy-minimization equilibria are presented for a hydrogen-helium plasma with $N(\text{He})/N(\text{H}) = 0.10$. These illustrate nicely the phenomena of pressure dissociation and ionization, and also demonstrate vividly the importance of choosing a reliable cutoff procedure for internal partition functions.

Subject headings: atomic processes — equation of state — stars: atmospheres

I. INTRODUCTION

In a previous paper (Hummer and Mihalas 1988, hereafter Paper I) we presented an analytical expression, differentiable to all orders, for the free energy of a multicomponent partially ionized plasma. In this theory continuous and differentiable bound-state partition functions are obtained by use of an occupation probability formalism, which accounts for perturbations by both charged and neutral perturbers. We showed that the theory can be made statistically mechanically consistent for perturbations by charged particles, and by neutral particles in the low-excitation limit. In addition, Däppen, Anderson, and Mihalas (1987) have shown that the occupation probabilities given in Paper I permit an accurate simulation of the radiation emitted from a precision plasma experiment (Wiese, Kelleher, and Paquette 1972).

The purpose of the present paper is threefold: (1) to document the mathematical details of our method, including a full set of explicit analytical expressions for all first and second derivatives required by the free-energy minimization procedure; (2) to describe the atomic and molecular data base that we have employed; and (3) to present some representative results for a hydrogen-helium mixture and show their sensitivity to the cutoff procedure used to truncate internal partition functions. A description of the calculation of

thermodynamic properties of the plasma will be given in a future paper (Däppen *et al.* 1988).

II. ALGORITHM

a) Free Energy

The free-energy minimization procedure is based on the "chemical picture" (Ebeling, Kraeft, and Kremp 1977), in which one identifies particle clusters (atoms, ions, molecules) as distinct particle species within the plasma. In terms of this picture, the free energy of a volume V of gas at temperature T can be written (Graboske, Harwood, and Rogers 1969; Paper I) as

$$F(T, V, \{N_s\}) = F_1 + F_2 + F_3 + F_4, \quad (1)$$

where

$$F_1 = -kT \sum_{s \neq e} N_s \left(\frac{3}{2} \ln T + \ln V - \ln N_s + \ln G_s + 1 \right), \quad (2)$$

$$F_2 = \sum_{s \neq e} N_s (E_{1s} - kT \ln Z_s^*), \quad (3)$$

$$F_3 = -kT N_e \left[\frac{2}{3} \frac{F_{3/2}(\eta)}{F_{1/2}(\eta)} - \eta \right], \quad (4)$$

and

$$F_4 = - \left(\frac{2\pi^{1/2} e^3}{3k^{1/2}} \right) \frac{1}{V^{1/2} T^{1/2}} \left(\sum_{\alpha} N_{\alpha} Z_{\alpha}^2 \theta_{\alpha} \right)^{3/2} \tau(x). \quad (5)$$

¹ The National Center for Atmospheric Research is sponsored by the National Science Foundation.

² Alexander von Humboldt Stiftung Senior US Scientist Awardee. Staff Member: Quantum Physics Division, National Bureau of Standards.

The occupation numbers $\{N_s\}$ are the number of particles of species s contained in volume V in thermodynamic equilibrium.

The term F_1 , in which

$$G_s \equiv (2\pi m_s k/h^2)^{3/2}, \quad (6)$$

accounts for the translational free energy of the atoms, ions, and molecules, which are assumed to behave as classical point particles.

The term F_2 gives the free energy associated with the internal excitation of species with excited states. The energy E_{1s} is the absolute energy of the ground state of species s , which corresponds to ionization stage j of chemical element k . For hydrogen, the zero point of the energy scale is taken to be the lowest vibration-rotation level of H_2 ; for all other elements it is the ground state of a neutral atom. In equation (3) Z_s^* is the modified internal partition function

$$Z_s^* \equiv \sum_i w_{is} g_{is} e^{-(E_{is} - E_{1s})/kT}, \quad (7)$$

where g_{is} and E_{is} are the statistical weight and energy of excitation state i of species s . As was shown in Paper I, the occupation probability w_{is} is given by

$$\ln w_{is} = -\left(\frac{4\pi}{3V}\right) \left\{ \sum_v N_v (r_{is} + r_{iv})^3 + 16 \left[\frac{(Z_s + 1)^{1/2} e^2}{K_{is}^{1/2} \chi_{is}} \right]^3 \sum_{\alpha \neq e} N_\alpha Z_\alpha^{3/2} \right\}. \quad (8)$$

In the first term, which represents a hard-sphere interaction between neutral particles, the index v runs over neutral particles only, and r_{ij} is the radius associated with state i of species j . This term is retained only if species s is neutral; exceptions to this rule are that it is used also if s corresponds to H^- or H_2^+ . In the second term, which accounts for perturbations by charged particles, the index α runs over all charged particles except electrons, Z_α is the net charge on ion species α , Z_s is the net charge on species s ($Z_s = 0$ for neutrals), χ_{is} is the ionization energy of level i , and K_{is} is a quantum correction of order unity (see Paper I). For particles with no internal structure (i.e., bare nuclei) we take $Z_\alpha^* \equiv g_{1\alpha} = 1$.

The term F_3 gives the free energy of an ideal gas of partially degenerate electrons. Here $F_n(\eta)$ is the standard Fermi-Dirac integral of order n (Cox and Giuli 1968, p. 793), and η is the degeneracy parameter, which is related to the number of electrons by

$$F_{1/2}(\eta) = \frac{\pi^{1/2}}{4G_e} \frac{N_e}{VT^{3/2}}. \quad (9)$$

Finally, the term F_4 accounts for the free energy of Coulomb interactions among all charged particles, including electrons, in the approximation used by Graboske, Harwood, and Rogers (1969). In equation (5) the sum on α runs over all charged species, and

$$\theta_e \equiv F_{-1/2}(\eta)/2F_{1/2}(\eta), \quad (10a)$$

$$\theta_\alpha \equiv 1 \quad (\alpha \neq e), \quad (10b)$$

$$\tau(x) \equiv 3x^{-3} [\ln(1+x) - x + \frac{1}{2}x^2], \quad (11)$$

and

$$x \equiv \left(\frac{2\pi^{1/2} e^3}{k^{3/2}} \right) \frac{1}{V^{1/2} T^{3/2}} \frac{F_{1/2}(\eta)}{F_{3/2}(\eta)} \left(\frac{\sum_{\alpha \neq e} N_\alpha Z_\alpha}{\sum_{\alpha \neq e} N_\alpha} \right) \times \left(\sum_\alpha N_\alpha Z_\alpha^2 \theta_\alpha \right)^{1/2}. \quad (12)$$

In this paper we omit all radiation terms (which are important contributors to the pressure and energy density at high temperatures and low densities) because they do not affect the equilibrium occupation numbers, which are our main interest here. It is trivial to include radiation effects because the radiation free energy is a function of T and V only, and simply adds linearly to the right-hand side of equation (1).

b) Minimization Procedure

To determine the equilibrium occupation numbers $\{N_s\}$ we must minimize $F(T, V, \{N_s\})$ with respect to all variations $\{\delta N_s\}$ permitted by the stoichiometric relations (which describe possible dissociation/ionization processes in the gas) and the constraints of number conservation and charge neutrality.

For hydrogen we consider the species H_2 , H_2^+ , H^- , H , and protons (p). The relevant stoichiometric equations are

$$\frac{\partial F}{\partial N_{H_2}} - 2 \frac{\partial F}{\partial N_H} = 0, \quad (13)$$

$$\frac{\partial F}{\partial N_{H_2^+}} - \frac{\partial F}{\partial N_H} - \frac{\partial F}{\partial N_p} = 0, \quad (14)$$

$$\frac{\partial F}{\partial N_{H^-}} - \frac{\partial F}{\partial N_H} - \frac{\partial F}{\partial N_e} = 0, \quad (15)$$

and

$$\frac{\partial F}{\partial N_H} - \frac{\partial F}{\partial N_p} - \frac{\partial F}{\partial N_e} = 0. \quad (16)$$

Let α_k be the fraction, by number, of all nuclei that belong to chemical element k (in any ionization stage), normalized such that

$$\sum_k \alpha_k = 1. \quad (17)$$

Then the total number of nuclei in volume V of a gas of density ρ is

$$N_{\text{tot}} = \rho V / \mu m_0, \quad (18)$$

where m_0 is one atomic mass unit, and the mean molecular weight is

$$\mu = \sum_k \alpha_k A_k, \quad (19)$$

where A_k is the atomic weight of element k . In practice we always choose $V = 1 \text{ cm}^{-3}$. The number conservation relation for hydrogen is then

$$2(N_{H_2} + N_{H_2^+}) + N_{H^-} + N_H + N_p = \alpha_H N_{\text{tot}}. \quad (20)$$

For all other elements we ignore molecule formation and treat only a ladder of J_k ionization stages ($J_k = Z_k + 1$, where Z_k is the nuclear charge of element k). Then for each element we have $J_k - 1$ ionization equations

$$\frac{\partial F}{\partial N_{jk}} - \frac{\partial F}{\partial N_{j+1,k}} - \frac{\partial F}{\partial N_e} = 0 \quad (j = 1, \dots, J_k - 1), \quad (21)$$

and a number conservation equation

$$\sum_{j=1}^{J_k} N_{jk} = \alpha_k N_{\text{tot}}. \quad (22)$$

Finally, the entire system is closed by the charge conservation

equation

$$N_{\text{H}2+} - N_{\text{H}^-} + N_p + \sum_k \sum_{j=1}^{j_k} (j-1)N_{jk} = N_e. \quad (23)$$

Equations (13)–(16) and (20)–(23) are nonlinear in $\{N_{sj}\}$, and must therefore be solved iteratively. Because we can write analytical expressions for both first and second derivatives of F with respect to the $\{N_s\}$ (see Appendix A), it is easy to use a Newton-Raphson scheme. Thus starting from a trial set $\{N_s^0\}$ of occupation numbers, we calculate $F(T, V, \{N_s^0\})$, $(\partial F/\partial N_s)^0$, and $(\partial^2 F/\partial N_s \partial N_t)^0$. Inserting these values in linearized versions of equations (13)–(16) and (20)–(23), we obtain a linear system for the corrections $\{\delta N_{sj}\}$ comprising dissociation and ionization equations of the form

$$\sum_s A_{rs} \sum_t \frac{\partial^2 F}{\partial N_s \partial N_t} \delta N_t = - \sum_s A_{rs} \frac{\partial F}{\partial N_s}, \quad (24)$$

and number and charge conservation equations of the form

$$\sum_s B_{re} \delta N_e = C_r - \sum_s B_{rs} N_s. \quad (25)$$

Here the sums on s run over all species, including electrons. We improve the numerical condition of equations (24) and (25) by additional procedures described below; they are then easily solved by standard techniques. For example, it is preferable in practice to solve for $\delta N_{sj}/N_s$ instead of δN_{sj} itself.

c) Numerical Details

i) Fermi-Dirac Integrals

The Fermi-Dirac integrals $F_{3/2}$, $F_{1/2}$, and $F_{-1/2}$ were computed using a subroutine FERDIR written by K. S. Kölbig for the CERN Computer Center Program Library. This subroutine is based on rational approximations by Cody and Thacher (1967); it provides results accurate to at least 10 significant digits in the domain of principal interest. The derivatives $F'_{-1/2}$ and $F''_{-1/2}$ were computed from formulae obtained by differentiating the approximation for $F_{-1/2}$ twice analytically. Note that the usual recursion formula connecting F'_k to F'_{k-1} breaks down when $k \leq \frac{1}{2}$; thus $F'_{-3/2}$ and $F'_{-5/2}$ do not exist, whereas $F'_{-1/2}$ and $F''_{-1/2}$ are bounded and well behaved because $F_{-1/2}(\eta)$ is holomorphic in η .

ii) Computational Strategy

The present code is designed to produce tables, rather than results for an arbitrary choice of $(\rho, T, \{\alpha_k\})$. Therefore, the code marches along an isotherm, starting from the lowest density point. This procedure is advantageous because purely temperature-dependent quantities can then be computed once and for all. At the lowest densities we use, nonideal effects are usually negligible, so it suffices to start the iteration procedure from the corresponding Saha equilibrium. At subsequent points we change $\log \rho$ by a constant increment, compute a new value for N_{tot} , and estimate starting values for the occupation numbers either by scaling those at the previous point on the isotherm by $(\rho_{\text{new}}/\rho_{\text{old}})$, or by using a linear extrapolation of the logarithms of the occupation numbers at the two previous points on the isotherm.

iii) Windowing

A characteristic feature of occupation numbers in a ionizing (or dissociating) gas is that the corresponding occupation fractions

$$f_{jk} \equiv N_{jk} / \sum_j N_{jk}, \quad (26)$$

typically vary by many orders of magnitude along an isotherm. Once a given f_{jk} drops below some minimum threshold (we use $f_{\text{min}} = 10^{-14}$), the contributions of that component of the gas to number or charge conservation gets lost in the roundoff, and the set of stoichiometric relations connecting that species to others may become ill conditioned. To avoid these problems, we choose a “window” containing all the dominant ionization (or dissociation) stages of each element, and discard (i.e., force to zero) the occupation numbers of all ion stages outside the window. For example, at moderate temperatures and low densities the window for, say, silicon might include Si I, Si II, Si III, and Si IV; as we move to higher densities along the isotherm, recombination occurs, so that at the highest densities the window might include only Si I and Si II. Similarly, at very high temperatures and low densities the window for, say, neon might include only Ne X and the bare ion Ne XI, but at much higher densities at the same temperature it might contain Ne I and Ne II. In practice we always retain at least one ion stage above and below the most abundant ion (if they exist physically).

The linearized reaction equations for discarded species are replaced by a one on the diagonal, and zeros elsewhere in the row and on the right-hand side, which guarantees $\partial N/N = 0$ for those species. This procedure significantly improves the stability and the accuracy of the solution, and eliminates physically unneeded ions (e.g., the highest ionization stages of, say, Fe at $\log T = 3.5$) from the computation. It is probably not necessary for a simple H–He mix, but becomes essential when many elements are included simultaneously.

iv) Convergence Criteria

To determine convergence we examine the occupation fractions f_{jk} . We demand that

$$\max_{(j,k)} |\delta f_{jk}| \leq \epsilon = 10^{-10} \quad (27)$$

for all species, including electrons (for which we take $f_e = N_e/N_{\text{tot}}$). Use of equation (27) gives us good control of the dominant ion stages of each chemical element. But it should be noted that for species for which f_{jk} becomes comparable to ϵ , the error in $\delta N_{jk}/N_{jk}$ may be considerably larger than ϵ ; these errors are, nevertheless, acceptable because such species are only minor players in determining ionization equilibrium, number conservation, and charge conservation. The code fails to converge altogether when the electron occupation fraction f_e drops below machine-word accuracy ($\sim 10^{-15}$). This problem, which occurs at the lowest temperatures and very (indeed unrealistically) high densities can be avoided by including a low ionization potential species such as K, or by accounting adequately for the effects of pressure ionization in neutral material (discussed in § IV and Appendix B).

Finally, it should be mentioned that very stringent tests, to be described in our next paper (Däppen *et al.* 1987), were applied to assure that the results produced by the code are correct.

III. ATOMIC AND MOLECULAR DATA BASE

a) Hydrogen

The following species of hydrogen are included in the calculation: H_2 , H_2^+ , H^- , H , and H^+ . A total of 284 vibration-rotation levels of the ground electronic state of H_2 were computed from the empirical anharmonic-oscillator and vibrating-rotator constants given by Herzberg and Howe

(1959). Initially another 28 excited electronic states (yielding a total of 6438 vibration-rotation levels) were also included, but it was found that these states are appreciably populated only when the dominant form of hydrogen is H; hence, they were dropped. For H_2^+ we computed a total of 443 vibration-rotation levels from constants given by Vardya (1966), which were adjusted slightly to give a good fit to theoretical energies of high vibration-rotation levels as given by Hunter, Yau, and Pritchard (1974).

For neutral hydrogen we used 100 distinct states specified by the principal quantum number n with energies calculated from the standard formulae. The dissociation and ionization energies we adopted for hydrogen species are listed in Table 1. Absolute energies E_{1s} of the ground state of each species relative to the ground level of H_2 are given in Table 2.

Estimates of atomic and molecular radii are required in order to calculate the neutral-neutral perturbation contained in equation (8). To calculate effective radii for H_2 we solved equations (11) and (12) of Vardya (1965) for each vibration-rotation level, using a Newton-Raphson iteration. The geometry assumed by Vardya implies that the effective collision radius between the atom and the center of the molecule is $(\frac{3}{4})r$. For H_2^+ we solved equations (9), (14), and (15) of Vardya (1966) for each vibration-rotation level. Here the assumed geometry implies that the effective collision radius is $0.433r$. For H^- we adopted a radius of 1.5 \AA based on the data by Pekeris (1962) and in the *Handbook of Chemistry and Physics* (Weast 1979). For H we used the formula

$$\langle r \rangle = (a_0/2Z)[3n^2 - l(l+1)] \quad (28)$$

for all excited states. For the ground state we adopted $r = a_0$ as a somewhat more conservative (i.e., smaller) estimate. The adopted ground-state radii for all species of H are shown in Table 3.

b) Other Elements

For He we made use of extensive NBS tables of energy levels supplemented with estimated values of quantum defects to fill in values for all (n, L, S) states with $n \leq 10$. Hydrogenic energies were used for $11 \leq n \leq 100$. Hydrogenic values were used throughout for $1 \leq n \leq 100$ of He^+ . Radii of the excited states of He were estimated from equation (28); for the ground state we adopted 0.5 \AA .

Although the data are not used in the calculations discussed in this paper, we mention that we have assembled a databank of $\sim 20,000$ energy levels for all ions of the astrophysically abundant (or otherwise important) elements C, N, O, Ne, Na, Mg, Al, Si, S, Ar, K, Ca, and Fe. These data will be used at a later time in calculations of various mixes.

TABLE 1
ADOPTED DISSOCIATION AND IONIZATION ENERGIES FOR SPECIES OF HYDROGEN

Species	Energy	Numerical Value (cm^{-1})
H_2	$D(H_2)$	36118.3
H_2^+	$D(H_2^+)$	21378.6
H^-	$D(H^-)$	6082.65
H	$I(H)$	109678.8

TABLE 2
ABSOLUTE GROUND STATE ENERGIES FOR SPECIES OF HYDROGEN

Species	E_{1s}	Numerical Value (cm^{-1})
H_2	0	0
H_2^+	$D(H_2) + I(H) - D(H_2^+)$	124418.5
H^-	$\frac{1}{2}D(H_2) - D(H^-)$	11976.5
H	$\frac{1}{2}D(H_2)$	18059.15
H^+	$\frac{1}{2}D(H_2) + I(H)$	127737.95

IV. RESULTS AND DISCUSSION

Using the free-energy minimization code described above we have calculated isotherms for several representative astrophysical mixtures. In this paper we restrict attention to only a hydrogen-helium mixture, having $N(\text{He})/N(\text{H}) = 0.1$, in the domain $-10 \leq \log \rho \leq +2$ and $3.5 \leq \log T \leq 7$. We focus exclusively on equilibrium populations and ionization fractions, and defer discussion of thermodynamic quantities and application to opacities to later papers.

Although the density domain where our equation of state will be used for opacity calculations in stellar envelopes is $\log \rho \leq -2$, we have pushed it to much higher densities in order to explore the effects of pressure dissociation and pressure ionization. Preliminary computations showed that in the low-temperature regime ($\log T \leq 4.75$) the occupation probabilities used in equation (8) do, in fact, produce pressure dissociation of H_2 for $\log \rho \geq -2$ but are unable to produce pressure ionization of neutral hydrogen atoms at yet higher densities. Instead, the plasma collapses into a dense neutral "jelly" in which every hydrogen nucleus is counted as a "neutral particle" with a "bound" electron even though its perturbed internal partition function is orders of magnitude smaller than the unperturbed ground-state statistical weight. This behavior is unphysical because in reality the atoms are so strongly perturbed that the electrons should be free in a Fermi gas, in which each electron may interact with several ions simultaneously. Fontaine, Graboske, and Van Horn (1977) similarly report that their free-energy minimization technique broke down for $\rho \geq 10^{-2}$ when $T \leq 10^5 \text{ K}$. In order to obtain at least a qualitatively reasonable pressure ionization effect we therefore introduced an additional configurational term, described in Appendix B, into the free energy. This term provides a stiffer neutral-neutral interaction (rising as the square of ξ , the ratio of the volume occupied by extended particles to the total available volume), and does lead to complete ionization of all components of the gas at sufficiently high densities ($\log \rho \geq 0$ for hydrogen). We emphasize that the results discussed below for the low-temperature high-density regime are qualitative and illustrative only. At higher temperatures ($\log T \geq 4.75$) there are always enough ions to assure pressure ionization at high densities through the destruction of bound states by perturbations by charged particles.

TABLE 3
ADOPTED RADII FOR SPECIES OF HYDROGEN

Species	Radius (\AA)
H_2	1.45
H_2^+	1.56
H^-	1.5
H	0.529

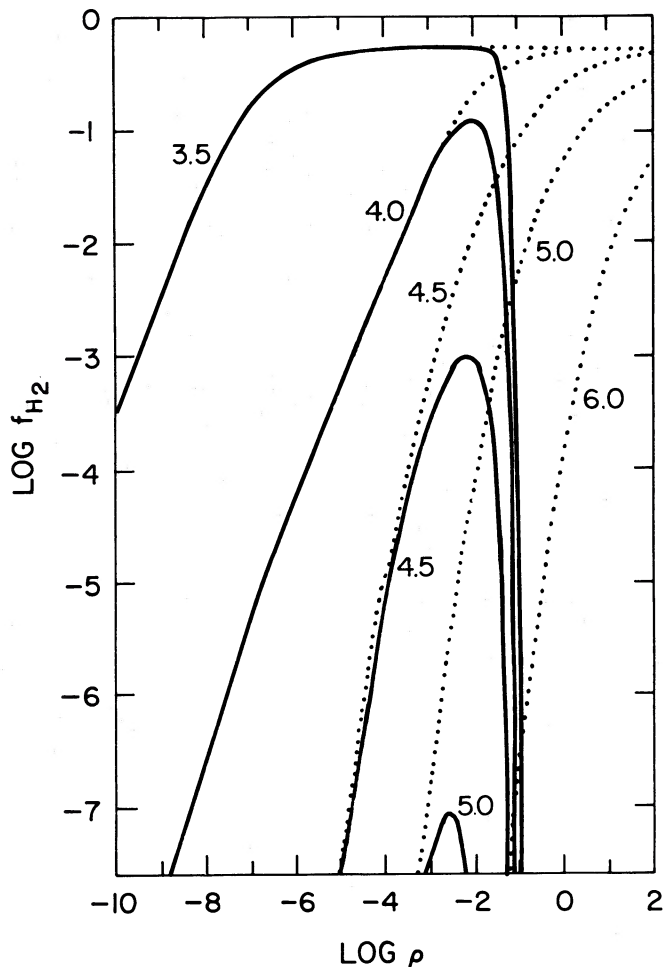


FIG. 1.—*Abscissa*: logarithm of density. *Ordinate*: logarithm of molecular hydrogen fraction $f_{H_2} \equiv N(H_2)/(\text{total number of hydrogen atoms})$. Note that $\log f_{H_2} = -0.3$ corresponds to all hydrogen bound into molecules. *Solid curves*: free-energy-minimization equilibrium using modified internal partition functions (FMIN). *Dotted curves*: Saha equilibrium using full internal partition functions for H_2 and H_2^+ , and ground states only for all other species (SAHAG). All curves are labeled with $\log T$.

Results for f_{H_2} , f_H , f_{He} , and f_{He+} are shown in Figures 1–4. In all of the figures the solid curves show the free-energy minimization equilibrium using modified internal partition functions (FMIN). Dashed curves show a Saha equilibrium (SAHAZ) using internal partition functions which include all bound states contained in the data base, i.e., a large but arbitrary number for all species. Dotted curves show a Saha equilibrium (SAHAG) using these internal partition functions only for H_2 and H_2^+ (which have a finite number of states), and only ground states for all other species. The density variation (i.e., slopes) of all the Saha curves in Figures 1–4 can be understood easily from simple analytical arguments; the behavior of the FMIN curves is more complex.

In Figure 1 we see that at sufficiently great densities a Saha equilibrium always leads to the physically absurd result of complete recombination of all the hydrogen into molecules no matter how high the temperature is. In contrast, in the FMIN equilibrium the neutral-neutral interactions in the occupation probability of equation (8) destroy all bound states of H_2 for $\log \rho \approx -1$, thereby forcing pressure dissociation of H_2 . (At high temperatures interactions with charged perturbers are

also important.) Thus at $\log T = 3.5$ we find that all hydrogen exists as H_2 for $\log \rho \geq -4$ until it pressure dissociates at $\log \rho \approx -1.5$. For $\log T \geq 4$ we find that the molecular hydrogen fraction reaches a maximum well below full recombination, and then decreases monotonically with increasing density.

In Figure 2 we see that Saha equilibrium predicts that at a given temperature the neutral hydrogen fraction becomes nearly unity at some density, and then declines at higher densities as H recombines into H_2 . For $\log T = 3.5$ and 4.0 there is no difference in f_H between the SAHAZ (*dashed curves*) and SAHAG (*dotted curves*) equilibria because these temperatures are too low to produce significant population of the excited states of H. But for $\log T \geq 4.5$ the excited states of H become heavily populated, and there is a huge discrepancy between the SAHAG and SAHAZ equilibria. For example, notice that f_H for the SAHAZ isotherm with $\log T = 7.0$ is nearly the same as f_H for the SAHAG isotherm with $\log T = 4.5$. Said differently, at the same temperature and density the neutral hydrogen fractions for the two sets of Saha equilibria can differ by as much as six orders of magnitude. This discrepancy results because hydrogen ionization is greatly decreased when a large number of excited states are available in neutral H; indeed, it

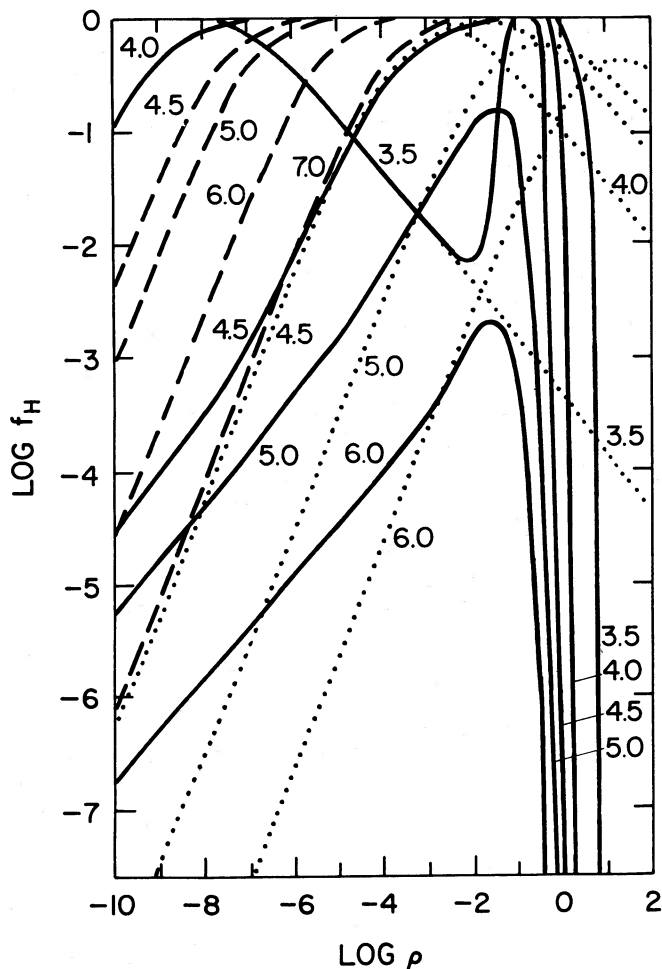


FIG. 2.—*Ordinate*: logarithm of neutral hydrogen fraction $f_H \equiv N(H)/(\text{total number of hydrogen atoms})$. *Dashed curves*: Saha equilibrium using full internal partition functions for all species (SAHAZ). *Abscissa*, *solid curves*, and *dotted curves*: as in Fig. 1.

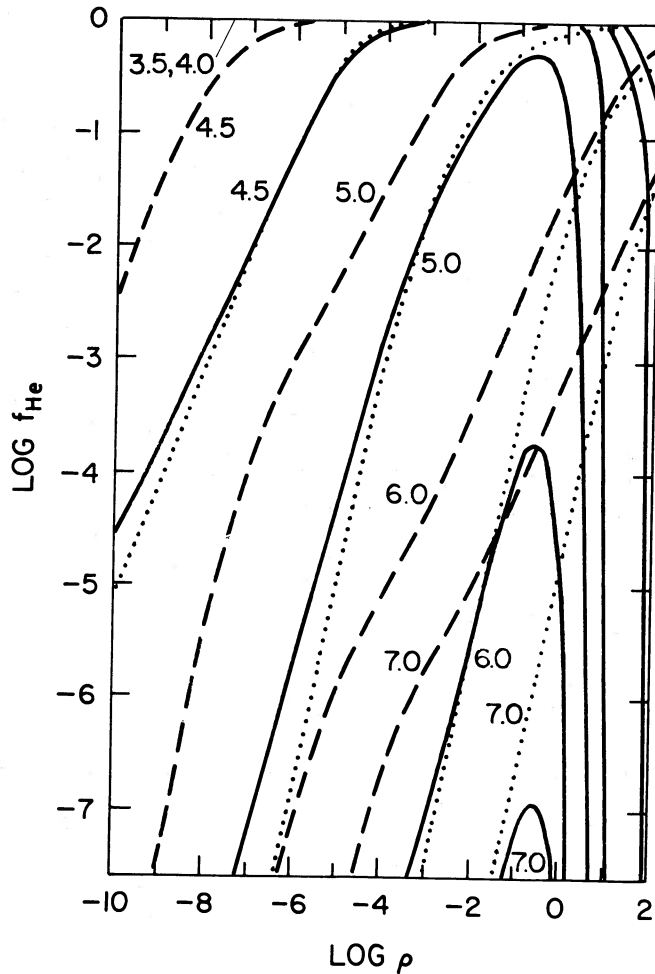


FIG. 3.—Ordinate: logarithm of neutral helium fraction $f_{\text{He}} \equiv N(\text{He})/[N(\text{He}) + N(\text{He}^+) + N(\text{He}^{++})]$. Abscissa, solid curves, dashed curves, and dotted curves: as in Figs. 1 and 2.

can be made arbitrarily large simply by including more bound states. It is thus clear that the choice of the number of states kept in an internal partition function is of central importance, and therefore that it is vital that the theory used to truncate internal partition functions be accurate.

For $\log T = 3.5$, the run of f_{H} for the FMIN equilibrium follows the SAHAG curve (which shows progressive recombination of H into H_2) until $\log \rho \approx -2$, at which point H_2 pressure dissociates and f_{H} rises back to unity on the range $-1 \leq \log \rho \leq 0$; at $\log \rho \approx 0$ the hydrogen atoms undergo pressure ionization, and f_{H} plummets. For $\log T = 4$, essentially all the hydrogen is H atoms for $-7 \leq \log \rho \leq -3$; for $-3 \leq \log \rho \leq -1.5$ the FMIN curve dips slightly as some H_2 forms and then pressure dissociates; for $-1.5 \leq \log \rho \leq -0.5$ the hydrogen is again all neutral atoms; and for $\log \rho \geq -0.5$ pressure ionization occurs and f_{H} drops to zero. The behavior of f_{H} for the other three isotherms shown is qualitatively identical; consider the case with $\log T = 6$. At densities lower than the lowest plotted, perturbations of bound states by neighboring particles become negligible; hence, the bound-state partition function becomes fully populated and the FMIN curve converges to the SAHAZ curve. At higher and higher densities, more and more bound states are destroyed, until finally only the ground state remains; the FMIN curve then crosses the

SAHAG curve (near $\log \rho = -3$). At yet higher densities the FMIN curve drops below the SAHAG curve as even the ground state becomes perturbed, until at some point ($\log \rho \approx -1.5$) perturbations destroy all the bound atoms and pressure ionization ensues.

Figure 3 shows the variation of f_{He} along several isotherms. For $\log T = 3.5$ and 4.0 both of the Saha equilibria predict that all of the helium remains neutral for $\log \rho \geq -10$. The FMIN results agree with the Saha results up to $\log \rho \approx +1$, at which point He abruptly pressure ionizes into He^+ . For $\log T \geq 4.5$ the behavior is qualitatively the same on all isotherms. Here both the SAHAG and SAHAZ equilibria predict eventual recombination to pure neutral He at sufficiently high densities for any temperature. Notice that the discrepancy between the SAHAG and SAHAZ curves is much smaller for He than for H. The reason is that the $\text{He} \leftrightarrow \text{He}^+$ equilibrium depends on the ratio of the partition functions for He and He^+ ; when excited states are included, both partition functions increase by a large factor, but their ratio changes relatively little by comparison. In contrast, for hydrogen the neutral atom has a partition function which can change by a large factor when excited states are included, but the (bare) ion has a fixed statistical weight; therefore the ratio of atomic to ionic partition function

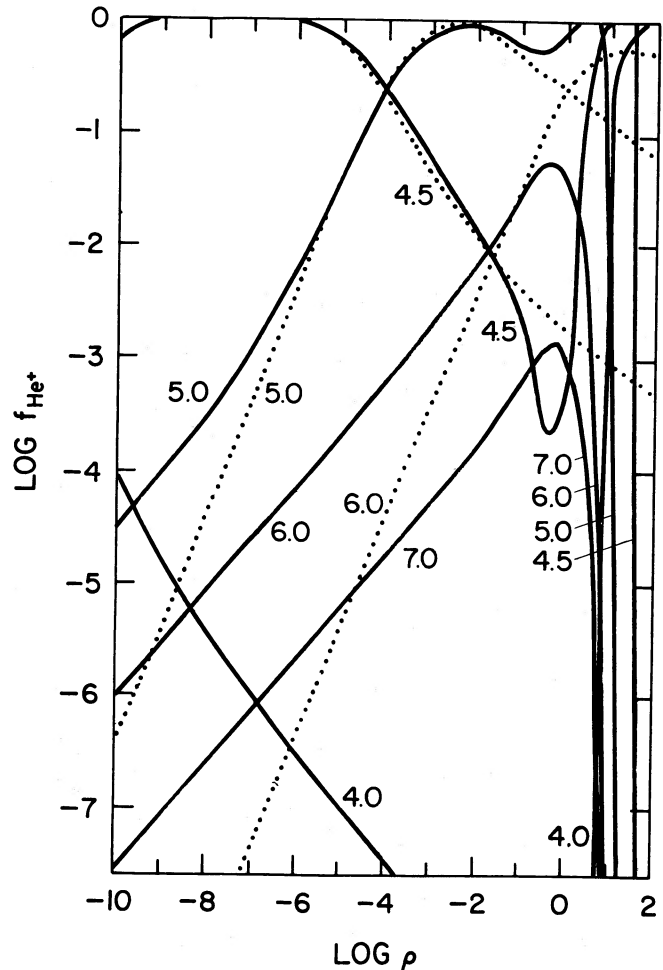


FIG. 4.—Ordinate: logarithms of ionized helium fraction $f_{\text{He}^+} \equiv N(\text{He}^+)/[N(\text{He}) + N(\text{He}^+) + N(\text{He}^{++})]$. Abscissa, solid curves, dashed curves, and dotted curves: as in Figs. 1 and 2.

can vary drastically between the SAHAG and SAHAZ cases. For $\log T \geq 4.5$ the FMIN results all show a rise to maximum, followed by abrupt pressure ionization at $\log \rho \sim 0$.

The variation of f_{He^+} shown in Figure 4 is qualitatively the same for the three SAHAG isotherms: f_{He^+} rises with increasing density as He^{++} recombines to form He^+ , reaches a maximum, and then declines as He^+ recombines to form He. The FMIN curves are more complicated. At $\log T = 4.0$, f_{He^+} declines for $-10 \leq \log \rho \leq 0$ as He^+ recombines to form He, then rises rapidly for $\log \rho \geq 1$ to a maximum at $\log \rho = 2$ as He pressure ionizes to He^+ . At yet higher densities f_{He^+} would decrease again as He^+ pressure ionizes to He^{++} . At $\log T = 4.5$, f_{He^+} is essentially unity for $\log \rho \leq -6$, drops to a minimum at $\log \rho \approx -0.5$ as He^+ recombines into He, returns to unity at $\log \rho \approx 1$ when He pressure ionizes, then drops sharply at $\log \rho = 1.5$ as He^+ pressure ionizes to He^{++} . At $\log T = 5$, f_{He^+} first rises with increasing density as He^{++} recombines to form He^+ , and reaches a maximum near unity at $\log \rho \approx -2.5$. It then declines as He^+ recombines to form He until pressure ionization of He into He^+ begins at $\log \rho \approx -0.5$ and drives f_{He^+} back to unity at $\log \rho \approx 0.5$; f_{He^+} then drops sharply as pressure ionization of He^+ occurs at $\log \rho \approx 1$. At yet higher temperatures the behavior is simpler: f_{He^+} first rises with increasing density as He^{++} recombines into He^+ , reaches a maximum well below unity, and then decreases sharply when pressure ionization converts He^+ into He^{++} .

We have checked our ionization fractions against results from a completely independently written Saha ionization equilibrium code in the appropriate (i.e., low-density) regime, and against other results (usually very sparse) published in the literature or made available by private communication. In all cases agreement was at least as good as the method of comparison would permit. Nevertheless, we would be happy to participate in joint efforts to make detailed comparisons with other codes.

V. CONCLUSION

The FMIN results presented above are based on a free-energy-minimization technique which accounts for (1) the translational free energy of classical point atoms, ions, and molecules; (2) the internal free energy of particles with multiple bound states; (3) the free energy of partially degenerate electrons; and (4) the configurational free energy of Coulomb interactions among charged particles. The internal partition functions are kept finite by use of an occupation probability

formalism which accounts for perturbation of bound states by both neutral and charged neighboring particles.

Our method successfully produces pressure dissociation and ionization in both neutral and partially ionized gases. To achieve pressure ionization in a completely neutral gas we are forced to introduce an additional configurational free energy, which mimics the second-order term in an expansion of the classical hard-sphere interaction. In the (ρ, T) regime where this additional term is important ($\log \rho \geq -1$ and $\log T \leq 4.75$) our results are only qualitative. In contrast, in all other regimes, where perturbations by charged particles dominate, our estimates of internal partition functions should be reasonably accurate, and ionization fractions (and other thermodynamic properties) should be reliable.

At low densities our FMIN results approach those given by a Saha equilibrium with full internal partition functions, and at high densities they approach those given by a Saha equilibrium with ground states only. This behavior is readily explained in terms of the destruction of bound states of an atom or ion by perturbations from neighboring particles. Furthermore, the large discrepancies between the two Saha equilibria show that it is essential to have the ability to calculate the internal partition functions accurately, i.e., to be able to determine reliably the total number of levels that remain bound in atoms and ions. We believe that the occupation probability method satisfies this requirement. In addition, the *qualitative* differences in behavior between the FMIN results and both sets of Saha results at high densities shows the great importance of accounting for pressure dissociation and ionization.

It is a great pleasure to thank Barbara Weibel Mihalas for a key suggestion that made the windowing procedure described in § II possible. D. G. H. wishes to thank the Alexander von Humboldt Stiftung for a US Senior Scientist Award. We thank Charles Prosser for his help in assembling the atomic data base used in these calculations, and R. Gilliland and C. J. Hansen for reading a draft of this paper and offering useful comments. The computations described in this paper were carried out at the National Center for Atmospheric Research and the National Center for Supercomputing Applications, both of which are sponsored by the National Science Foundation. This work was supported in part by National Aeronautics and Space Administration grant NAGW-766 to the University of Colorado and National Science Foundation grant AST 85-19209 to the University of Illinois.

APPENDIX A

DERIVATIVES OF THE FREE ENERGY WITH RESPECT TO OCCUPATION NUMBERS

In this appendix we present a complete collection of analytical expressions for the derivatives needed to carry out the free energy minimization procedure. While they are straightforward to derive in principle, the algebra is tedious and error prone, and we believe that they will be useful to other workers in this field. Additional derivatives needed for the calculation of thermodynamic quantities will be given in the next paper of this series.

I. TRANSLATIONAL FREE ENERGY

For any particles (r, s) other than electrons

$$\frac{\partial F_1}{\partial N_s} = -kT \left(\frac{3}{2} \ln T + \ln V - \ln N_s + \ln G_s \right), \quad (\text{A1})$$

and

$$\frac{\partial^2 F_1}{\partial N_r \partial N_s} = \frac{kT}{N_s} \delta_{rs}, \quad (\text{A2})$$

while for electrons (e),

$$\frac{\partial F}{\partial N_e} = \frac{\partial^2 F_1}{\partial N_e^2} = \frac{\partial^2 F_1}{\partial N_e \partial N_s} \equiv 0. \quad (\text{A3})$$

II. INTERNAL FREE ENERGY

We assume that the occupation probability w_{is} depends only on the occupation numbers $\{N_r\}$ and the volume V , and is independent of the temperature T . Then for $r \neq e$ and $q \neq e$

$$\frac{\partial F_2}{\partial N_r} = E_{1r} - kT \ln Z_r^* - kT \sum_{s \neq e} \frac{N_s}{Z_s^*} \frac{\partial Z_s^*}{\partial N_r}, \quad (\text{A4})$$

and

$$\frac{\partial^2 F_2}{\partial N_r \partial N_q} = -kT \left[\frac{1}{Z_r^*} \frac{\partial Z_r^*}{\partial N_q} + \frac{1}{Z_q^*} \frac{\partial Z_q^*}{\partial N_r} + \sum_{s \neq e} \frac{N_s}{Z_s^*} \left(\frac{\partial^2 Z_s^*}{\partial N_r \partial N_q} - \frac{1}{Z_s^*} \frac{\partial Z_s^*}{\partial N_r} \frac{\partial Z_s^*}{\partial N_q} \right) \right], \quad (\text{A5})$$

while for electrons

$$\frac{\partial F_2}{\partial N_e} = \frac{\partial^2 F_2}{\partial N_r \partial N_e} = \frac{\partial^2 F_2}{\partial N_e^2} \equiv 0. \quad (\text{A6})$$

To calculate derivatives of the partition function we use the identities

$$\frac{\partial w}{\partial x} = w \frac{\partial \ln w}{\partial x}, \quad (\text{A7})$$

and

$$\frac{\partial^2 w}{\partial x \partial y} = w \left(\frac{\partial^2 \ln w}{\partial x \partial y} + \frac{\partial \ln w}{\partial x} \frac{\partial \ln w}{\partial y} \right), \quad (\text{A8})$$

to write, for any variables x and y other than T ,

$$\frac{\partial Z_s^*}{\partial x} = \sum_i \left(\frac{\partial \ln w_{is}}{\partial x} \right) w_{is} g_{is} e^{-(E_{is} - E_{1s})/kT}, \quad (\text{A9})$$

$$\frac{\partial^2 Z_s^*}{\partial x \partial y} = \sum_i \left(\frac{\partial^2 \ln w_{is}}{\partial x \partial y} + \frac{\partial \ln w_{is}}{\partial x} \frac{\partial \ln w_{is}}{\partial y} \right) w_{is} g_{is} e^{-(E_{is} - E_{1s})/kT}. \quad (\text{A10})$$

In turn

$$\frac{\partial \ln w_{is}}{\partial N_v} = - \left(\frac{4\pi}{3V} \right) (r_{is} + r_{1v})^3, \quad (\text{A11})$$

where v corresponds to a neutral species and s to a neutral species or H_2^+ or H^- ,

$$\frac{\partial \ln w_{is}}{\partial N_\alpha} = - \left(\frac{4\pi}{3V} \right) 16 \left[\frac{(Z_s + 1)^{1/2} e^2}{K_{is}^{1/2} \chi_{is}} \right]^3 Z_\alpha^{3/2}, \quad (\text{A12})$$

where α corresponds to a charged species (other than electrons), and

$$\frac{\partial^2 \ln w_{is}}{\partial N_q \partial N_r} \equiv 0 \quad (\text{A13})$$

for all (q, r) . Equation (A13) provides a valuable simplification that makes the evaluation of equation (A10) much easier.

III. FREE ENERGY OF PARTIALLY DEGENERATE ELECTRONS

For partially degenerate electrons

$$\frac{\partial F_3}{\partial N_e} = \eta kT, \quad (\text{A14})$$

$$\frac{\partial^2 F_3}{\partial N_e^2} = \frac{2kT}{N_e} \frac{F_{1/2}(\eta)}{F_{-1/2}(\eta)} = \frac{kT}{N_e \theta_e}, \quad (\text{A15})$$

and

$$\frac{\partial F_3}{\partial N_s} = \frac{\partial^2 F_3}{\partial N_s^2} = \frac{\partial^2 F_3}{\partial N_s \partial N_e} \equiv 0. \quad (\text{A16})$$

In addition

$$\frac{\partial \eta}{\partial N_s} \equiv 0 \quad (s \neq e), \quad (\text{A17})$$

$$\frac{\partial \eta}{\partial N_e} = \frac{2F_{1/2}(\eta)}{N_e F_{-1/2}(\eta)} = \frac{1}{N_e \theta_e}, \quad (\text{A18})$$

and

$$\frac{\partial^2 \eta}{\partial N_e^2} = -\frac{F'_{-1/2}(\eta)}{F_{-1/2}(\eta)} \left(\frac{\partial \eta}{\partial N_e} \right)^2. \quad (\text{A19})$$

IV. CONFIGURATIONAL FREE ENERGY OF COULOMB INTERACTIONS

Let the subscripts (α, β, γ) refer to charged particles only. Then for the free energy of Coulomb interactions we have

$$\frac{\partial F_4}{\partial N_\beta} = F_4 \left(\frac{3}{2} \frac{Z_\beta^2}{\sum_\alpha N_\alpha Z_\alpha^2 \theta_\alpha} + \frac{\tau'}{\tau} \frac{\partial x}{\partial N_\beta} \right) \quad (\beta \neq e), \quad (\text{A20})$$

$$\frac{\partial^2 F_4}{\partial N_\beta \partial N_\gamma} = \frac{1}{F_4} \frac{\partial F_4}{\partial N_\beta} \frac{\partial F_4}{\partial N_\gamma} + F_4 \left\{ \left[\frac{\tau''}{\tau} - \left(\frac{\tau'}{\tau} \right)^2 \right] \frac{\partial x}{\partial N_\beta} \frac{\partial x}{\partial N_\gamma} + \left(\frac{\tau'}{\tau} \right) \frac{\partial^2 x}{\partial N_\beta \partial N_\gamma} - \frac{3}{2} \frac{Z_\beta^2 Z_\gamma^2}{(\sum_\alpha N_\alpha Z_\alpha^2 \theta_\alpha)^2} \right\} \quad (\beta \neq e, \gamma \neq e), \quad (\text{A21})$$

$$\frac{\partial F_4}{\partial N_e} = F_4 \left[\frac{3}{2} \frac{\theta_e + N_e \theta'_e (\partial \eta / \partial N_e)}{\sum_\alpha N_\alpha Z_\alpha^2 \theta_\alpha} + \frac{\tau'}{\tau} \frac{\partial x}{\partial N_e} \right], \quad (\text{A22})$$

$$\frac{\partial^2 F_4}{\partial N_\beta \partial N_e} = \frac{1}{F_4} \frac{\partial F_4}{\partial N_\beta} \frac{\partial F_4}{\partial N_e} + F_4 \left\{ \left[\frac{\tau''}{\tau} - \left(\frac{\tau'}{\tau} \right)^2 \right] \frac{\partial x}{\partial N_\beta} \frac{\partial x}{\partial N_e} + \left(\frac{\tau'}{\tau} \right) \frac{\partial^2 x}{\partial N_\beta \partial N_e} - \frac{3}{2} \frac{Z_\beta^2 [\theta_e + N_e \theta'_e (\partial \eta / \partial N_e)]}{(\sum_\alpha N_\alpha Z_\alpha^2 \theta_\alpha)^2} \right\}, \quad (\text{A23})$$

and

$$\frac{\partial^2 F_4}{\partial N_e^2} = \frac{1}{F_4} \left(\frac{\partial F_4}{\partial N_e} \right)^2 + F_4 \left[\left[\frac{\tau''}{\tau} - \left(\frac{\tau'}{\tau} \right)^2 \right] \left(\frac{\partial x}{\partial N_e} \right)^2 + \left(\frac{\tau'}{\tau} \right) \frac{\partial^2 x}{\partial N_e^2} + \frac{3}{2} \frac{\theta_e'' N_e \left(\frac{\partial \eta}{\partial N_e} \right)^2 + \theta_e' \left(2 \frac{\partial \eta}{\partial N_e} + N_e \frac{\partial^2 \eta}{\partial N_e^2} \right) - \frac{[\theta_e + N_e \theta'_e (\partial \eta / \partial N_e)]^2}{\sum_\alpha N_\alpha Z_\alpha^2 \theta_\alpha} \right]. \quad (\text{A24})$$

Here

$$\theta'_e = \theta_e \left[\frac{F'_{-1/2}(\eta)}{F_{-1/2}(\eta)} - \theta_e \right], \quad (\text{A25})$$

$$\theta''_e = \theta_e \left[\frac{F''_{-1/2}(\eta)}{F_{-1/2}(\eta)} - 3\theta'_e - \theta_e^2 \right], \quad (\text{A26})$$

$$\theta'_\alpha = \theta''_\alpha \equiv 0, \quad \alpha \neq e, \quad (\text{A27})$$

and

$$\tau' = -\frac{3}{x} \left(\tau - \frac{1}{1+x} \right), \quad (\text{A28})$$

$$\tau'' = -\frac{1}{x} \left[4\tau' + \frac{3}{(1+x)^2} \right]. \quad (\text{A29})$$

Further

$$\frac{\partial x}{\partial N_\beta} = x \left(\frac{Z_\beta}{\sum_{\alpha \neq e} N_\alpha Z_\alpha} - \frac{1}{\sum_{\alpha \neq e} N_\alpha} + \frac{1}{2} \frac{Z_\beta^2}{\sum_\alpha N_\alpha Z_\alpha^2 \theta_\alpha} \right) \quad (\beta \neq e), \quad (\text{A30})$$

$$\frac{\partial^2 x}{\partial N_\beta \partial N_\gamma} = \frac{1}{x} \frac{\partial x}{\partial N_\beta} \frac{\partial x}{\partial N_\gamma} + x \left[\frac{-Z_\beta Z_\gamma}{(\sum_{\alpha \neq e} N_\alpha Z_\alpha)^2} + \frac{1}{(\sum_{\alpha \neq e} N_\alpha)^2} - \frac{1}{2} \frac{Z_\beta^2 Z_\gamma^2}{(\sum_\alpha N_\alpha Z_\alpha^2 \theta_\alpha)^2} \right] \quad (\beta \neq e, \gamma \neq e), \quad (\text{A31})$$

$$\frac{\partial x}{\partial N_e} = x \left\{ \frac{[\theta_e + N_e \theta'_e (\partial \eta / \partial N_e)]}{2 \sum_{\alpha} N_{\alpha} Z_{\alpha}^2 \theta_{\alpha}} - \frac{3 F_{1/2}(\eta)}{2 F_{3/2}(\eta)} \frac{\partial \eta}{\partial N_e} + \frac{1}{N_e} \right\}, \quad (\text{A32})$$

$$\frac{\partial^2 x}{\partial N_{\beta} \partial N_e} = \frac{1}{x} \frac{\partial x}{\partial N_{\beta}} \frac{\partial x}{\partial N_e} - \frac{x Z_{\beta}^2 [\theta_e + N_e \theta'_e (\partial \eta / \partial N_e)]}{2 (\sum_{\alpha} N_{\alpha} Z_{\alpha}^2 \theta_{\alpha})^2}, \quad (\text{A33})$$

and

$$\frac{\partial^2 x}{\partial N_e^2} = \frac{1}{x} \left(\frac{\partial x}{\partial N_e} \right)^2 + x \left[-\frac{1}{N_e^2} - \frac{3 F_{1/2}(\eta)}{2 F_{3/2}(\eta)} \left\{ \frac{\partial^2 \eta}{\partial N_e^2} + \left(\frac{\partial \eta}{\partial N_e} \right)^2 \left[\theta_e - \frac{3 F_{1/2}(\eta)}{2 F_{3/2}(\eta)} \right] \right\} + \frac{1}{2 \sum_{\alpha} N_{\alpha} Z_{\alpha}^2 \theta_{\alpha}} \left\{ \theta_e'' N_e \left(\frac{\partial \eta}{\partial N_e} \right)^2 + \theta_e' \left(2 \frac{\partial \eta}{\partial N_e} + N_e \frac{\partial^2 \eta}{\partial N_e^2} \right) - \frac{[\theta_e + N_e \theta'_e (\partial \eta / \partial N_e)]^2}{\sum_{\alpha} N_{\alpha} Z_{\alpha}^2 \theta_{\alpha}} \right\} \right]. \quad (\text{A34})$$

APPENDIX B

PRESSURE IONIZATION IN NEUTRAL GASES

As was noted in § IV, the neutral-neutral perturbations contained in equation (8) are adequate to pressure-dissociate H_2 , but fail to produce pressure ionization of H or He at low temperatures. The basic reason for this failure is that at the temperatures and densities of relevance the electrons are strongly degenerate; it is therefore energetically more favorable for electrons to be counted as "bound" than to overcome the Fermi energy in the free electron gas. In contrast, dissociation proceeds without difficulty because no free electron is produced, hence no degeneracy barrier is encountered.

In Paper I we pointed out that our neutral-neutral interaction term is only linear in ξ , the ratio of the volume filled by particles having extended radii to the total volume; hence, that it cannot be expected to be accurate as ξ approaches unity. More rigorous expressions for the free energy of a hard-sphere gas contain logarithmic or rational polynomial singularities as $\xi \rightarrow 1$; see e.g., equations (6.4) and (6.8) of Graboske, Harwood, and Rogers (1969). Those singularities prevent a collapse of a partially ionized plasma to a dense neutral state, and guarantee that as the density increases, a free-energy minimum with the gas partially or completely ionized can always be found. However, these expressions are difficult to implement numerically because as the occupation numbers fluctuate in the Newton-Raphson iteration, the arguments of some of the terms may be driven into a forbidden domain, and the free energy driven through the singularity, thus disrupting the calculation.

We have therefore examined the effects of a simple, nonsingular, and differentiable supplement to our original neutral-neutral interaction term. To provide a rationale for our choice, start with the classical free energy of a hard-sphere gas:

$$F_5 = -kT \sum_i N_i \ln \left[1 - \left(\frac{2\pi}{3V} \right) \sum_j N_j (R_i + R_j)^3 \right]. \quad (\text{B1})$$

Expanding to first order we obtain

$$F_5 \approx kT \sum_i N_i \left(\frac{4\pi}{3V} \right) \sum_j \frac{1}{2} N_j (R_i + R_j)^3, \quad (\text{B2})$$

which, to within a factor of 2 in density, is what one obtains from equations (7) and (8) and the definition $F = -kT \ln Z$ if one assumes that all states of the atom or ion are perturbed by the same amount as the ground state (i.e., replace w_{is} in eq. [7] by w_{1s}).

This correspondence suggests that we supplement equation (8) by a term resembling the next (quadratic) term in the expansion of equation (B1). Thus defining

$$\xi_v = \left(\frac{4\pi}{3V} \right) \sum_{\mu} N_{\mu} (r_{1\mu} + r_{1\nu})^3, \quad (\text{B3})$$

we expect the next term to be of the general form

$$\tilde{F} = -kT \sum_{\nu} N_{\nu} (-C \xi_{\nu}^2), \quad (\text{B4})$$

where C is a numerical constant. In equations (B3) and (B4) the indices μ and ν range over neutral particles (and H^- and H_2^+) only. Thus for the purpose of numerical experimentation we have taken the additional free energy to be

$$F' = -kT \sum_{\nu} N_{\nu} \ln \Psi_{\nu}, \quad (\text{B5})$$

where

$$\ln \Psi_{\nu} \equiv -\alpha \xi_{\nu}^n. \quad (\text{B6})$$

Equations (B3), (B5), and (B6) are equivalent to multiplying the occupation numbers of all states in the internal partition function of species ν by an additional occupation probability $\exp(-\alpha \xi_{\nu}^n)$. Because Ψ_{ν} depends only on ground-state radii, it remains essentially unity until the density gets so high that even the ground state is perturbed.

In the computations discussed in this paper we used $n = 2$ and $\alpha = 10$; this value for α is much larger than the correct coefficient of the quadratic term in the expansion of equation (B1). The effect of F' becomes noticeable for $\xi \sim 0.3$, and strongly dominates as $\xi \rightarrow 1$. In principle, one could calibrate the choice of α and n by using experimental data for dense hydrogen plasmas; unfortunately we do not know of any data of this kind. In practice the choices we have made for α and n produce pressure ionization very efficiently once F' becomes comparable to F_1 through F_4 .

The derivatives of F' are straightforward. One finds

$$\frac{\partial F'}{\partial N_\nu} = -kT \left(\ln \Psi_\nu + \sum_\lambda N_\lambda \frac{\partial \ln \Psi_\lambda}{\partial N_\nu} \right), \quad (\text{B7})$$

and

$$\frac{\partial^2 F'}{\partial N_\mu \partial N_\nu} = -kT \left(\frac{\partial \ln \Psi_\nu}{\partial N_\mu} + \frac{\partial \ln \Psi_\mu}{\partial N_\nu} + \sum_\lambda N_\lambda \frac{\partial^2 \ln \Psi_\lambda}{\partial N_\mu \partial N_\nu} \right), \quad (\text{B8})$$

where

$$\frac{\partial \ln \Psi_\nu}{\partial N_\nu} = \frac{n \ln \Psi_\lambda}{\xi_\lambda} \left(\frac{4\pi}{3V} \right) (r_{1\lambda} + r_{1\nu})^3, \quad (\text{B9})$$

and

$$\frac{\partial^2 \ln \Psi_\lambda}{\partial N_\mu \partial N_\nu} = \frac{n-1}{n \ln \Psi_\lambda} \frac{\partial \ln \Psi_\lambda}{\partial N_\mu} \frac{\partial \ln \Psi_\lambda}{\partial N_\nu}. \quad (\text{B10})$$

The pressure ionization produced by F' is quite abrupt. It is therefore essential to have good starting values for occupation numbers if the Newton-Raphson iteration is to converge. To obtain these estimates we precede the Newton-Raphson step by a binary chop procedure that scans for the minimum of the free energy as ionization fractions are varied between 0 and 1; the scan is continued until the relevant ionization fraction is determined to within ± 0.001 in the logarithm. We found it satisfactory to vary the ionization fractions one at a time, first scanning $\text{H} \rightarrow \text{H}^+$, then $\text{He} \rightarrow \text{He}^+$. We believe that a sequential scan procedure will also work in a gas composed of several elements if one proceeds from the most abundant to the least abundant element in order.

In general, the method outlined above has performed reliably, but it appears that the computation, as implemented, may suffer from severe numerical calculations, or a mild instability, because relatively minor algebraic rearrangements of terms can sometimes lead to divergence of the iteration procedure. In addition, even though occupation fractions, such as those shown in Figures 1–4, always vary smoothly, thermodynamic quantities (e.g., χ_ρ , c_ν , Γ_1 , etc.), which are more demanding on the quality of the solution, are sometimes noisy in the part of the (ρ, T) domain where F' dominates. Thus unless our code contains an undetected error, it seems that a computationally more rugged method for forcing pressure ionization in a low-temperature neutral gas is still needed.

REFERENCES

- Cody, W. J., and Thacher, H. C. Jr. 1967, *Math Comp.*, **21**, 30.
 Cox, J. P., and Giuli, R. T. 1968, *Principles of Stellar Structure*, Vol. 1, (New York: Gordon & Breach), p. 793.
 Däppen, W., Anderson, L. S., and Mihalas, D. 1987, *Ap. J.*, **319**, 195.
 Däppen, W., Mihalas, D., Hummer, D. G., and Mihalas, B. W. 1988, *Ap. J.*, **332**, in press (Paper III).
 Ebeling, W., Kraeft, W. D., and Kremp, D. 1977, *Theory of Bound States and Ionization Equilibrium in Plasmas and Solids* (Berlin: Akademie).
 Fontaine, G., Graboske, H. C., and Van Horn, H. M. 1977, *Ap. J. Suppl.*, **35**, 293.
 Graboske, H. C., Harwood, D. J., and Rogers, F. J. 1969, *Phys. Rev.*, **186**, 210.
 Herzberg, G., and Howe, L. L. 1959, *Canadian J. Phys.*, **37**, 636.
 Hummer, D. G., and Mihalas, D. 1988, *Ap. J.*, **331**, 794 (Paper, I).
 Hunter, G., Yau, A. W., and Pritchard, H. O. 1974, *Atomic Data Nucl. Data Tables*, **14**, 11.
 Pekeris, C. L. 1962, *Phys. Rev.*, **126**, 1470.
 Vardya, M. S. 1965, *M.N.R.A.S.*, **129**, 345.
 ———. 1966, *M.N.R.A.S.*, **134**, 183.
 Weast, R. C. 1979, *Handbook of Chemistry and Physics* (Boca Raton: Chemical Rubber Press), p. F-214.
 Wiese, W. L., Kelleher, D. E., and Paquette, D. R. 1972, *Phys. Rev. A*, **6**, 1132.

W. DÄPPEN: Observatoire de Paris-Meudon, 92195 Meudon, France

D. G. HUMMER and D. MIHALAS: Joint Institute for Laboratory Astrophysics, University of Colorado, Boulder, CO 80309